BARYON/CHARGE CUMULANT RATIO AT SECOND ORDER*

Masakiyo Kitazawa

Yukawa Institute for Theoretical Physics, Kyoto University
Kyoto 606-8502, Japan
and
J-PARC Branch, KEK Theory Center, Institute of Particle and Nuclear Studies
KEK, 319-1106 Japan
and
Department of Physics, Osaka University, Toyonaka, Osaka, 560-0043 Japan

ShinIchi Esumi, Toshihiro Nonaka

Tomonaga Center for the History of the Universe, University of Tsukuba
Tsukuba, Ibaraki, 305-8751, Japan

Received 15 August 2022, accepted 14 October 2022,
published online 14 December 2022

Fluctuations of conserved charges are important probes to explore a hot and dense medium in relativistic heavy-ion collisions. In this paper, we focus on the experimentally-observed second-order cumulants of baryon number and electric charge at the top RHIC energy. We compare the ratio of these cumulants with the corresponding susceptibility ratio observed in lattice QCD numerical simulations. We show that, if one assumes that the experimental results on the cumulants are thermal, the "temperature" predicted from this comparison is significantly lower than that of the chemical freezeout. We argue that this discrepancy comes from the diffusion and resonance decays. The importance of the acceptance correction of the transverse-momentum cut is also emphasized.

DOI:10.5506/APhysPolBSupp.16.1-A82

1. Introduction

Fluctuations of conserved charges are useful observables for investigating phase transitions in the hot medium created by relativistic heavy-ion collisions (HIC) [1–3]. In particular, the higher-order cumulants characterizing non-Gaussianity of fluctuations are known to behave more anomalously

* Presented at the 29th International Conference on Ultrarelativistic Nucleus–Nucleus Collisions: Quark Matter 2022, Kraków, Poland, 4–10 April, 2022.

around the phase boundary [4–6], which would be used for the signal of the phase transitions. Suggestive non-monotonic behaviors as functions of $\sqrt{s_{NN}}$ have been reported in recent experiments [7, 8].

In the present study [9], we investigate the ratio of the second-order cumulants of net-baryon number and net-electric charge, $\langle N_B^2\rangle_{\rm c}$ and $\langle N_Q^2\rangle_{\rm c}$, using the experimental results in Au+Au central collisions at $\sqrt{s_{NN}} = 200$ GeV by the STAR Collaboration [8, 10]. An advantage to focus on this quantity is that it is composed only of the second-order cumulants so that various ambiguities in the experimental analyses that are more amplified for higher-order cumulants, such as systematic uncertainties from the efficiency correction [11], are suppressed in this ratio. From the experimental data for the most central (0–5%) collisions, we obtain the ratio by performing the reconstruction of baryon number cumulants [12] and the correction of the finite acceptance in the transverse momentum, $p_{\rm T}$, space.

We then compare the ratio with the result in the hadron resonance gas (HRG) model and the lattice QCD simulations. Provided that the experimentally-observed fluctuations are emitted from a thermal medium, the comparison shows the temperature $T \simeq 134$–138 MeV, which is significantly lower than the chemical freezeout temperature $T_{\rm chem}$.

2. Analysis of the cumulant ratio

We construct $\langle N_B^2\rangle_{\rm c}$ from the data on the proton number cumulants in Ref. [8] according to the procedure in Ref. [12], while we use the data from Ref. [10] for $\langle N_Q^2\rangle_{\rm c}$. The effects of the detector's efficiencies are corrected in these results.

The measurements in Refs. [8, 10] are performed within a finite $p_{\rm T}$-acceptance. Due to the acceptance the particles in the final state are observed only with imperfect probabilities

$$R_{p_{\rm T}} = \frac{(\text{particle number in } p_{\rm T}\text{-acceptance})}{(\text{total particle number})}\,. \tag{1}$$

Table 1. Ratio of the particle abundance in the $p_{\rm T}$-acceptance $R_{p_{\rm T}}$ obtained by the Blast-wave model.

Particle species ($p_{\rm T}$ range)	$R_{p_{\rm T}}$
Pions ($0.4 < p_{\rm T} < 1.6$ GeV)	0.44
Kaons ($0.4 < p_{\rm T} < 1.6$ GeV)	0.71
Protons ($0.4 < p_{\rm T} < 1.6$ GeV)	0.71
$\pi + K + p$ ($0.4 < p_{\rm T} < 1.6$ GeV)	0.49
Protons ($0.4 < p_{\rm T} < 2.0$ GeV)	0.82

Using the Blast-wave model with the parameters determined from the experimental data [13], the values of R_{p_T} for individual particles are obtained as shown in Table 1 for the p_T-acceptances in Refs. [8, 10]. We perform this correction for the p_T-acceptance using the same procedure as the efficiency correction assuming the binomial distribution [1, 12].

3. Results

In Fig. 1, we show the second-order cumulants $\langle N_B^2\rangle_\mathrm{c}$, $\langle N_Q^2\rangle_\mathrm{c}$, as well as that of the proton number $\langle N_p^2\rangle_\mathrm{c}$, divided by the rapidity window Δy as functions of Δy. These quantities are constant if they are generated from a thermal system having the boost invariance [1]. In the left panel, the triangles show $\langle N_p^2\rangle_\mathrm{c}/\Delta y$ from Ref. [8]. The dashed line near the data shows the total particle number $\langle N_p^{(\mathrm{total})}\rangle/\Delta y$. The squares in the same panel show $\langle N_B^2\rangle_\mathrm{c}/\Delta y$ obtained with the procedure from Ref. [12], while the circles show $\langle N_B^2\rangle_\mathrm{c}/\Delta y$ for which the p_T-acceptance correction is performed. The error bars show the statistical errors, which are negligibly small in these results. The dashed lines near these results are the total baryon number $\langle N_B^{(\mathrm{total})}\rangle/\Delta y = 2\langle N_p^{(\mathrm{total})}\rangle/\Delta y$. One sees that the deviation of $\langle N_B^2\rangle_\mathrm{c}$ from $\langle N_B^{(\mathrm{total})}\rangle$ at large Δy is pronounced by the corrections. This result is reasonable since the incomplete measurement tends to make the distribution close to the Skellam distribution in which $\langle N_B^2\rangle_\mathrm{c} = \langle N_B^{(\mathrm{total})}\rangle$ [1].

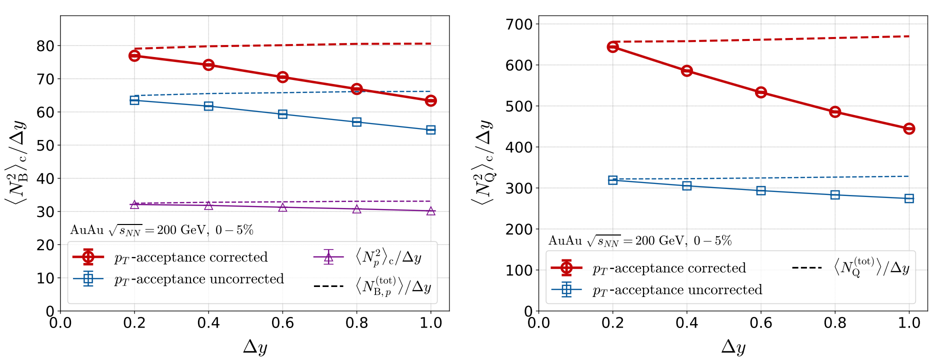

Fig. 1. Second-order cumulants $\langle N_B^2\rangle_\mathrm{c}$, $\langle N_p^2\rangle_\mathrm{c}$, and $\langle N_Q^2\rangle_\mathrm{c}$ divided by Δy obtained from the experimental results from Refs. [8, 10] at $\sqrt{s_{NN}} = 200$ GeV. The circle and square symbols show the results with and without the p_T-acceptance correction, respectively. The triangles in the right panel show $\langle N_p^2\rangle_\mathrm{c}/\Delta y$. The dashed lines near the symbols are the corresponding total particle numbers.

Shown in the right panel of Fig. 1 are $\langle N_Q^2\rangle_{\rm c}/\Delta y$ with (circles) and without (squares) the $p_{\rm T}$-acceptance correction. The meaning of the dashed lines is the same as in the left panel. The panel shows that the effect of the $p_{\rm T}$-acceptance correction is more significant than $\langle N_B^2\rangle_{\rm c}$ due to the smaller $R_{p_{\rm T}}$ for the electric charge.

In the left panel of Fig. 2, we show the $p_{\rm T}$-acceptance-corrected result of $\langle N_B^2\rangle_{\rm c}/\langle N_Q^2\rangle_{\rm c}$ with the circles. The dashed lines show $\langle N_B^{\rm (total)}\rangle/\langle N_Q^{\rm (total)}\rangle$. The shaded band represents the systematic errors that account for the propagation from that of $\langle N_B^2\rangle_{\rm c}$ in Ref. [8]; we, however, note that this error band should be regarded only as a guide since the estimate of the systematic errors of $\langle N_B^2\rangle_{\rm c}/\langle N_Q^2\rangle_{\rm c}$ needs detailed knowledge of the experimental analyses. In the panel, the result without the $p_{\rm T}$-acceptance correction is also shown by the squares as reference. One sees that the correction strongly modifies the ratio.

If fluctuations are emitted from a thermal system having a boost invariance, the ratio $\langle N_B^2\rangle_{\rm c}/\langle N_Q^2\rangle_{\rm c}$ is a constant as a function of Δy [1]. While $\langle N_B^2\rangle_{\rm c}/\Delta y$ and $\langle N_Q^2\rangle_{\rm c}/\Delta y$ become decreasing functions when the effects of the global charge conservation are taken into account, this Δy dependence cancels out in the ratio $\langle N_B^2\rangle_{\rm c}/\langle N_Q^2\rangle_{\rm c}$ for the thermal case. On the other hand, from the left panel of Fig. 2, one sees that the acceptance-corrected ratio has a clear increasing trend as a function of Δy. This result shows that the fluctuations in the HIC are not emitted from a purely thermal system including the effect of global conservation.

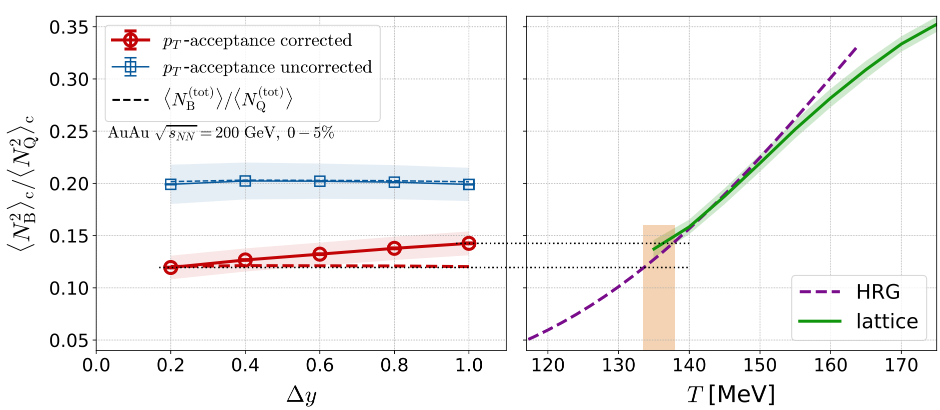

Fig. 2. Left panel shows the ratio $\langle \delta N_B^2\rangle/\langle \delta N_Q^2\rangle$ obtained from the HIC as a function of the rapidity window Δy. The right panel shows the ratio obtained in the lattice QCD simulations [14] and the HRG model. The dotted horizontal lines and shaded area are for a comparison of the two results.

4. Comparison with HRG model and lattice results

Assuming that the fluctuations observed in the HIC are those of a thermal system, one can estimate the temperature of the system by comparing the ratio of cumulants with the results obtained in lattice QCD simulations. Even when the fluctuations are not thermal, such a comparison is useful for investigating the nature of the fluctuations.

To perform the comparison using the ratio $\langle N_B^2\rangle_c/\langle N_Q^2\rangle_c$, in the right panel of Fig. 2, we show the T dependence of $\langle N_B^2\rangle_c/\langle N_Q^2\rangle_c$ obtained from a lattice QCD simulation [14] by the solid line with an error band. Finite-volume effects of $\langle N_Q^2\rangle_c$ are corrected according to Ref. [14]. The range of the vertical axis is the same as in the left panel. The lattice results on thermodynamics are known to be well reproduced by the HRG model at low T. In the panel, the ratio $\langle N_B^2\rangle_c/\langle N_Q^2\rangle_c$ obtained in the HRG model is shown by the dashed line, where we use the set of hadrons in "QMHRG2020" [14] for the HRG model. The figure shows that the lattice result agrees well with the HRG model for $T \lesssim 145$ MeV, which suggests the validity of the latter in this range of T. From the panel, one also finds that $\langle N_B^2\rangle_c/\langle N_Q^2\rangle_c$ behaves almost linearly as a function of T in the range of T shown in the panel, which is an attractive feature of this ratio.

To compare the results in the left and right panels, in Fig. 2, we show the dotted horizontal lines at the values of $\langle N_B^2\rangle_c/\langle N_Q^2\rangle_c$ obtained from the HIC at $\Delta y = 0.2$ and 1.0. By comparing these values with the ratio in the HRG model, one finds that the temperature extracted from the naïve comparison gives $T \simeq 134$–138 MeV depending on Δy as shown by the shaded box in the right panel. We note that this temperature is significantly smaller than the chemical freezeout temperature $T_{\rm chem} \simeq 156$ MeV for $\sqrt{s_{NN}} = 200$ GeV [13]. The value of $\langle N_B^2\rangle_c/\langle N_Q^2\rangle_c$ in the HIC itself is about twice smaller than the value in the HRG model at $T = T_{\rm chem}$.

5. Summary

In the present study, we have investigated the cumulant ratio $\langle N_B^2\rangle_c/\langle N_Q^2\rangle_c$ observed in the HIC. Since this ratio consists only of the second-order conserved-charge cumulants, various uncertainties in the experimental measurement that are amplified for higher-order cumulants are suppressed in its analysis. The ratio in the HIC at $\sqrt{s_{NN}} = 200$ GeV is estimated from the experimental results by the STAR Collaboration [8, 10]. In addition to the reconstruction of the baryon number cumulant from those of protons, the effects of $p_{\rm T}$-acceptance are corrected. Our result shows that this correction strongly modifies the resulting values of the cumulants and their ratio and thus is crucial. Since the effect of the correction becomes more significant for higher-order cumulants [11], this result also shows the importance of the correction in their analysis for the search for the QCD critical point.

The naïve comparison of the obtained ratio with the HRG model suggests the temperature $T \simeq 134$–138 MeV, which is significantly lower than $T_{\rm chem}$. By taking this result seriously, it is suggested that the fluctuation observables in the HIC are generated in the hadronic phase later than the chemical freezeout.

However, we emphasize that this comparison is made assuming that the fluctuations in the HIC are thermal. On the other hand, the existence of the Δy dependence of $\langle N_B^2\rangle_{\rm c}/\langle N_Q^2\rangle_{\rm c}$ shows the violation of this assumption in the HIC. Therefore, to understand the experimental result correctly, one needs further investigations on the nature of fluctuations especially taking their dynamics into account [15]. The modifications of the cumulants due to the use of (pseudo-)rapidity in place of spacetime rapidity [16] and the resonance decays after the chemical freezeout are other important effects to be considered since they tend to make $\langle N_Q^2\rangle_{\rm c}$ larger and suppress $\langle N_B^2\rangle_{\rm c}/\langle N_Q^2\rangle_{\rm c}$. Since these effects are suppressed by extending Δy [1], the measurement of the fluctuations with larger Δy is an important experimental subject for resolving these issues.

REFERENCES

[1] M. Asakawa, M. Kitazawa, *Prog. Part. Nucl. Phys.* **90**, 299 (2016).

[2] A. Bzdak *et al.*, *Phys. Rep.* **853**, 1 (2020).

[3] M. Bluhm *et al.*, *Nucl. Phys. A* **1003**, 122016 (2020).

[4] S. Ejiri, F. Karsch, K. Redlich, *Phys. Lett. B* **633**, 275 (2006).

[5] M.A. Stephanov, *Phys. Rev. Lett.* **102**, 032301 (2009).

[6] M. Asakawa, S. Ejiri, M. Kitazawa, *Phys. Rev. Lett.* **103**, 262301 (2009).

[7] STAR Collaboration (J. Adam *et al.*), *Phys. Rev. Lett.* **126**, 092301 (2021).

[8] STAR Collaboration (M. Abdallah *et al.*), *Phys. Rev. C* **104**, 024902 (2021).

[9] M. Kitazawa, S. Esumi, T. Nonaka, `arXiv:2205.10030 [hep-ph]`.

[10] STAR Collaboration (J. Adam *et al.*), *Phys. Rev. C* **100**, 014902 (2019); *Erratum ibid.* **105**, 029901 (2022).

[11] T. Nonaka, M. Kitazawa, S. Esumi, *Phys. Rev. C* **95**, 064912 (2017); *Erratum ibid.* **103**, 029901 (2021); *Nucl. Instrum. Methods Phys. Res. A* **906**, 10 (2018).

[12] M. Kitazawa, M. Asakawa, *Phys. Rev. C* **85**, 021901 (2012); **86**, 024904 (2012).

[13] STAR Collaboration (B.I. Abelev *et al.*), *Phys. Rev. C* **79**, 034909 (2009).

[14] HotQCD Collaboration (D. Bollweg *et al.*), *Phys. Rev. D* **104**, 074512 (2021).

[15] M. Kitazawa, M. Asakawa, H. Ono, *Phys. Lett. B* **728**, 386 (2014); M. Kitazawa, *Nucl. Phys. A* **942**, 65 (2015).

[16] Y. Ohnishi, M. Kitazawa, M. Asakawa, *Phys. Rev. C* **94**, 044905 (2016).